University of Groningen

Myocardial extracellular volume fraction to differentiate healthy from cardiomyopathic myocardium using dual-source dual-energy CT

Abadia, Andres F.; van Assen, Marly; Martin, Simon S.; Vingiani, Vincenzo; Griffith, L. Parkwood; Giovagnoli, Dante A.; Bauer, Maximilian J.; Schoepf, U. Joseph

IMPORTANT NOTE: You are advised to consult the publisher's version (publisher's PDF) if you wish to cite from it. Please check the document version below.

Document Version
Publisher's PDF, also known as Version of record

Publication date:
2020

Link to publication in University of Groningen/UMCG research database

Research paper

Myocardial extracellular volume fraction to differentiate healthy from cardiomyopathic myocardium using dual-source dual-energy CT

Andres F. Abadia[a], Marly van Assen[a,b], Simon S. Martin[a,c], Vincenzo Vingiani[a],
L. Parkwood Griffith[a], Dante A. Giovagnoli[a], Maximilian J. Bauer[a], U. Joseph Schoepf[a,*]

[a] *Division of Cardiovascular Imaging, Department of Radiology and Radiological Science, Medical University of South Carolina, USA*
[b] *Department of Radiology, University Medical Center Groningen, Groningen, the Netherlands*
[c] *Department of Diagnostic and Interventional Radiology, University Hospital Frankfurt, Frankfurt, Germany*

ABSTRACT

Objective: To evaluate the feasibility of dual-energy CT (DECT)-based iodine quantification to estimate myocardial extracellular volume (ECV) fraction in patients with and without cardiomyopathy (CM), as well as to assess its ability to distinguish healthy myocardial tissue from cardiomyopathic, with the goal of defining a threshold ECV value for disease detection.

Methods: Ten subjects free of heart disease and 60 patients with CM (mean age 66.4 ± 9.4; 59 males and 11 females; 40 ischemic and 20 non-ischemic CM) underwent late iodine enhanced DECT imaging. Myocardial iodine maps were obtained using 3-material decomposition. ECV of the left ventricle was estimated from hematocrit levels and the iodine maps using the AHA 16-segment model. Receiver operating characteristic curve analysis was performed, with corresponding area under the curve, along with Youden's index assessment, to establish a threshold for CM detection.

Results: The median ECV for healthy myocardium, non-ischemic CM, and ischemic CM were 25.4% (22.9–27.3), 38.3% (33.7–43.0), and 36.9% (32.4–41.1), respectively. Healthy myocardium showed significantly lower ECV values compared to ischemic and non-ischemic CM ($p < 0.001$). From Youden's index analysis, an ECV > 29.5% would indicate the presence of CM in the myocardium (sensitivity = 90.3; specificity = 90.3); the AUC for this criterion was 0.950 ($p < 0.001$).

Conclusion: The findings of this study resulted in a statistically significant distinction between healthy myocardium and CM ECVs. This led to the establishment of a promising threshold ECV value that could facilitate the differentiation between healthy and diseased myocardium, and highlights the potential of this DECT methodology to detect cardiomyopathic tissue.

1. Introduction

Cardiomyopathy (CM) is a clinical diagnosis associated with muscular or electrical dysfunction of the heart, and often leads to cardiovascular death or progressive heart failure-related disability.[1,2] CM, especially dilated CM, is the third leading cause of heart failure in the United States[2]; therefore, its noninvasive assessment, and the ability to distinguish it from healthy myocardial tissue, would have significant clinical utility.

Myocardial fibrosis represents an important hallmark of myocardial damage in CM.[3,4] The assessment of myocardial extracellular volume

(ECV) fraction has been studied as a new approach toward the noninvasive evaluation of myocardial fibrosis, as ECV is increased in association with fibrosis.[4] Currently, cardiac magnetic resonance imaging (MRI) is the reference standard for the noninvasive assessment of ECV and is increasingly used to differentiate the etiology of CM.[5–7] However, this imaging technique is limited in its availability and has some known contraindications and limitations. Compared to MRI, CT offers a faster, more widely available, and cheaper acquisition, as well as the potential to scan patients with metal implants, the simultaneous assessment of coronary anatomy, and the potential for submillimeter resolution.[8,9] Previous studies have shown that ECV can be successfully measured

---

Abbreviations

AUC	Area Under the Curve
CAD	Coronary Artery Disease
CCTA	Cardiac Computed Tomography Angiography
CM	Cardiomyopathy
CTDI$_{vol}$	Volumetric Computed Tomography Dose Index
DECT	Dual-energy Computed Tomography
DLP	Dose-length Product
ECG	Electrocardiogram
ECV	Extracellular Volume
HCT	Hematocrit

HU	Hounsfield Units
ICD	Implantable Cardioverter Defibrillator
ICM	Ischemic Cardiomyopathy
IQR	Interquartile Range
LGE	Late Gadolinium Enhancement
LV	Left Ventricle
MRI	Magnetic Resonance Imaging
NICM	Non-ischemic Cardiomyopathy
ROC	Receiver Operating Characteristic
ROI	Region of Interest
SD	Standard Deviation
SECT	Single-energy Computed Tomography

---

with single-energy computed tomography (SECT) and dual-energy CT (DECT) with a high correlation between ECV measurements derived from CT, histologic quantification, and equilibrium MRI.[4,8,10–12]

More recently, a study demonstrated that ECV can be measured using a DECT approach with only a delayed iodine-enhanced acquisition.[9] As per the study, this approach provides similar results when compared to multiphase SECT, whilst lowering the radiation dose to the patient by replacing a true non-contrast scan with a virtual non-contrast DECT reconstruction.[9] This is possible given that with DECT, the system can be operated at different tube potentials, leading to maximum spectral separation, which results in optimal material differentiation.[13–15] This allows for different image reconstructions, such as a virtual-non contrast acquisition from the enhanced images, as well as iodine maps, which are important tools that aid in tissue characterization.[9,16,17] We propose to eliminate the need for a non-contrast acquisition (virtual or true) altogether by directly using the iodine concentration from the iodine maps, requiring only one image reconstruction.

The purpose of this study, thus, was to explore the potential of DECT to retrospectively quantify myocardial ECV, using iodine maps only, in patients with and without CM and assess its ability to distinguish healthy myocardial tissue from cardiomyopathic, with the goal of defining a threshold ECV value for disease detection. Although previous studies have explored the image-based measurement of ECV with different end-goals,[4,8–12] to the best of our knowledge, no other studies have utilized this methodology to define an ECV threshold for CM detection.

2. Methods

2.1. Study population

This study was approved by the Institutional Review Board and written informed consent was obtained from all subjects. The study was conducted in compliance with the Health Insurance Portability and Accountability Act. The subjects' clinical history, medical records, and image findings were reviewed to ascertain their health status and to screen for either healthy cardiac function or history of CM. To select our CM subjects, we analyzed data of patients who underwent a cardiac CT angiography (CCTA), as well as a delayed DECT scan, between 2008 and 2019 for the evaluation of suspected coronary artery disease (CAD) or known CM. Presence or absence of CM was further validated via an MRI perfusion scan with late gadolinium enhancement (LGE), which served as the reference standard. Twenty patients were identified with non-ischemic CM (NICM) and 40 with ischemic CM (ICM). Ten healthy subjects were included to serve as a control group, who had no signs of CM or ischemia on cardiac MRI, and underwent additional DECT delayed imaging. A total of 70 subjects were analyzed in our study (mean age 66.4 ± 9.4, 59 males and 11 females).

2.2. Image acquisition

All healthy subject DECT examinations were performed with a second-generation dual-source CT system (Somatom Definition Flash; Siemens Healthineers, Forchheim, Germany) between 2008 and 2014. CM subject examinations were performed with a third-generation dual-source CT system (Somatom Force; Siemens Healthineers) as the scanner was replaced at the end of 2014. From the entire imaging protocol the patients were subjected to, this study only used the contrast-enhanced delayed DECT acquisition: prospective electro-cardiogram (ECG) triggering, tube voltage and current, 100/140 kVp with 165 reference mA/rotation (second-generation) and 90/150 kVp with tin filtration and 90 mA/rotation (third-generation), gantry rotation time 280 ms/250 ms (second/third-generation), heart rate dependent pitch 0.2–0.43, and 1.5 mm section thickness with 1 mm overlap reconstructed in 60–75% diastole. Delayed acquisitions were obtained 7 min after the administration of 70 mL of iopromide (370 mg Iodine/mL; Ultravist, Bayer, Wayne, NJ), injected at a flow rate of 5.0 mL/s using a dual-syringe injector (Stellant, Bayer) and automated bolus triggering. Contrast injection was followed by a 50 mL saline flush. Contrast timing was automatically determined using a dedicated bolus tracking software application (CareBolus, Siemens Healthineers) with a region of interest (ROI) placed in the descending aorta, at the level of the carina. A trigger threshold level of 100 HU with a 4s delay was then selected for detection of bolus arrival.

2.3. ECV measurement on DECT-derived iodine maps

Iodine maps were derived from the DECT data on a commercially available 3D workstation (syngo.via VB10B, Siemens Healthineers) using a dedicated post-processing software (heart PBV, Siemens Healthineers), which is based on the 3-material decomposition method.[10,15] After the iodine maps were obtained, the images were reformatted to the short-axis plane, and ROIs were manually drawn on the myocardium using the American Heart Association's 16-segment model of the left ventricle (LV) (apex was excluded) (Fig. 1). Additionally, a circular ROI (at least 1.5 cm^2 in area) was drawn in the LV cavity to measure the iodine content in the blood-pool. ROIs with significant metal artifact interference were carefully avoided. Once iodine content (in mg/mL) was recorded from all the ROIs, the ECV fraction per segment was calculated taking into account the current (not older than 1 month from DECT acquisition) hematocrit (HCT) value as follows:

$$ECV = (1 - HCT)\frac{Iodine_{Myocardium}}{Iodine_{Bloodpool}}$$

2.4. Statistical analysis

All statistical analyses were performed using MedCalc (version 18.11.6, MedCalc Software bvba, Ostend, Belgium). To test for normal
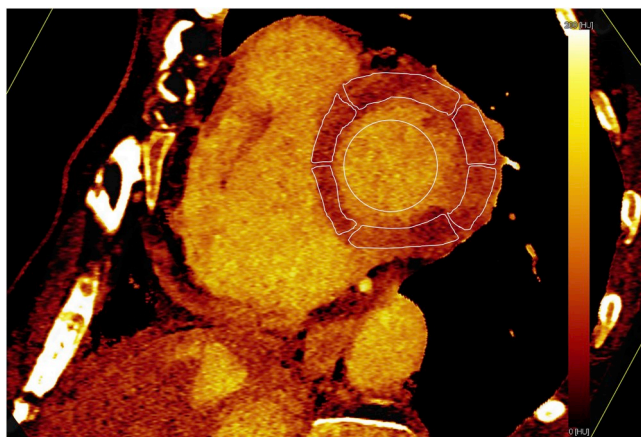
Fig. 1. Example of iodine map obtained with delayed contrast-enhanced DECT acquisition and illustration of AHA LV segmentation.

distribution, the D'Agostino-Pearson test was utilized; based on the results, non-parametric continuous variables were expressed as median with associated interquartile ranges (IQR) and parametric continuous variables were expressed as mean ± standard deviation (SD). Categorical variables were expressed as absolute numbers and percentages (n (%)). An independent Mann-Whitney U test was used to compare the baseline characteristics of healthy, ICM, and NICM subjects; the same test was used to assess the differences between ECV in healthy myocardium vs. ICM, healthy vs. NICM, and ICM vs. NICM. Additionally, receiver operating characteristic (ROC) curve analysis was performed, with corresponding area under the curve (AUC), in conjunction with Youden's index assessment, to determine whether this method of ECV calculation could differentiate between healthy myocardial tissue and cardiomyopathic, and establish a threshold for CM detection. ROC with AUC was also used to assess whether this methodology could differentiate between ICM and NICM. A p-value < 0.05 was considered statistically significant.

3. Results

3.1. Study population

The baseline characteristics of the study population are summarized in Table 1. There were no significant differences observed in patient demographics with the exception of HCT values, which were higher in healthy subjects vs. CM ones ($p = 0.0157$). The median volume CT dose index ($CTDI_{vol}$) for all study subjects was 16.0 mGy (IQR, 13.9–18.4) and the median dose-length product (DLP) was 258.2 mGy cm (IQR, 198.4–300.4).

None of the healthy subjects had cardiac assist devices in place while 95% (19/20) of NICM and 97.5% (39/40) of ICM did. Individual ROI segments with significant metal artifact interference were carefully avoided (n = 116 segments were adjusted accordingly). The analysis of this study thus encompassed a total of 1004 ECV measurements (155 ROIs in healthy subjects, 308 in NICM, and 541 ICM).

3.2. Myocardial ECV measurements

Healthy myocardium ECV values (median 25.4%; IQR, 22.9–27.3) were significantly lower than CM (median 37.4%; IQR, 32.8–41.6) ($p < 0.001$); additionally, there was a significant difference observed between NICM ECVs (median 38.3%; IQR, 33.7–43.0) and ICM ECVs (median 36.9%; IQR, 32.4–41.1) ($p = 0.003$). These results are illustrated in Fig. 2 which displays a per-layer analysis (basal, mid-ventricular, and apical) and a per-segment analysis of median ECVs obtained across the study. From the first analysis (per-layer), it can be observed that ECVs were consistently higher in the NICM population vs. ICM ECVs, and both of these were much higher than the ECVs in healthy subjects. From the second analysis (per-segment), NICM ECVs were higher vs. ICM in 12 out of the 16 segments, while both were still consistently higher against the healthy ECVs in all segments. Fig. 3 shows a histogram of all the ECV measurements taken in this study (1004) and illustrates the distribution of values.

3.3. ROC analysis

The results from ROC curve analysis (with corresponding AUC), in conjunction with Youden's index assessment (i.e. criterion, sensitivity, and specificity), are illustrated in Fig. 4. From Youden's index analysis, an ECV > 29.5% would indicate the presence of CM (vs. healthy) in the myocardium (sensitivity = 90.3; specificity = 90.3); the associated AUC for this criterion was 0.950 ($p < 0.001$). The same analysis also suggests an ECV > 39.6% to indicate the presence of NICM (vs. ICM) (sensitivity = 41.9; specificity = 69.3); however, the associated AUC for this criterion was only 0.560 ($p = 0.004$).

4. Discussion

In this study we evaluated the feasibility of using iodine concentrations, obtained from a single delayed contrast-enhanced DECT acquisition, to calculate ECV with the goal of defining a threshold value to distinguish healthy myocardial tissue from cardiomyopathic. The median ECV values for healthy myocardium found by our simplified approach were consistent with previously published values obtained with CT and MRI.[10,18,19] There was a clear distinction between ECVs for healthy myocardium and CM ECVs. Youden's index analysis suggests that an ECV > 29.5% would indicate the presence of CM. The sensitivity and specificity associated with this threshold, along with the accompanying high AUC, illustrates the capability of this methodology to distinguish healthy from cardiomyopathic tissue; however, its ability to differentiate types of CM is not as dependable. Although the difference observed between ECVs from NICM and ICM was statistically significant, the low AUC obtained from ROC analysis suggests that the likelihood of distinguishing between these 2 types of CM is almost equally probable.

A recent study evaluated the feasibility of equilibrium contrast material-enhanced DECT to determine ECV in NICM compared with MRI and applied the results in healthy subjects vs NICM patients.[10] We believe our investigation differs from the aforementioned study in several aspects: 1) we analyzed the ECV differences between healthy

Table 1
Baseline characteristics of the study population.

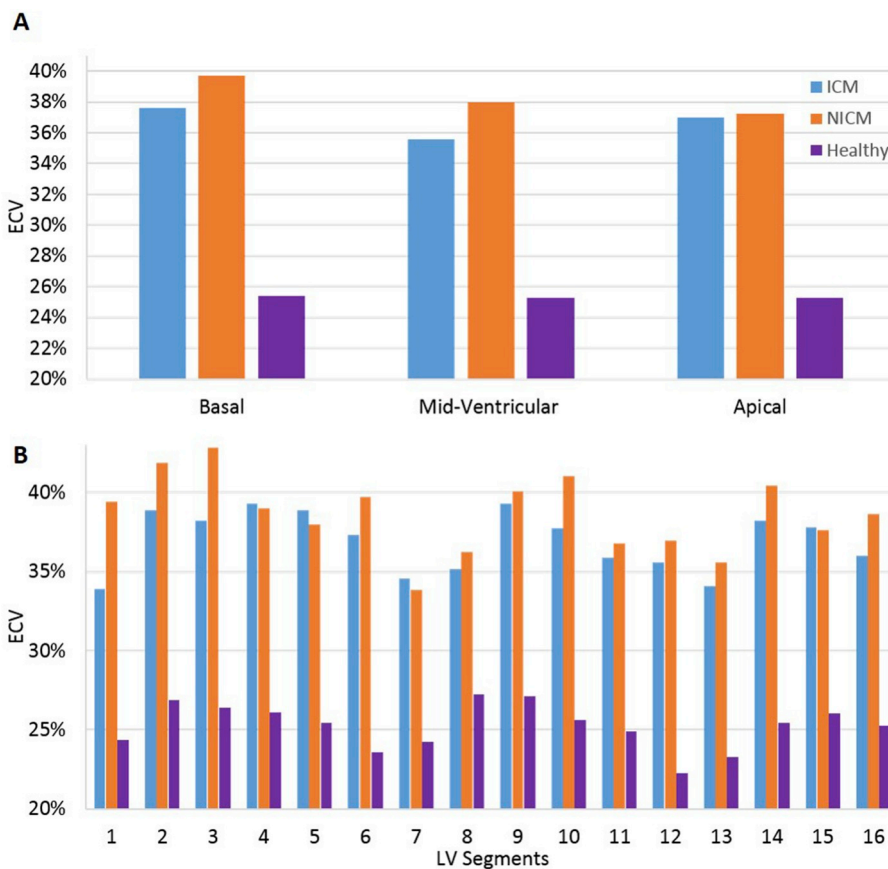|	Healthy Subjects (n = 10)	NICM (n = 20)	ICM (n = 40)
Age (y)	60.6 ± 9.2	63.9 ± 10.3	69.1 ± 8.1
No. of men*	7 (70.0)	15 (75.0)	37 (92.5)
BMI (kg/m^2)	29.6 (28.9–32.1)	29.5 (28.3–35.7)	28.6 (25.6–31.8)
Heart rate (bpm)	74.0 (70.8–78.8)	68.5 (60.0–77.3)	60.0 (60.0–69.3)
Hematocrit (%)	42.3 (41.7–43.15)	37.6 (34.7–40.5)	39.1 (35.7–41.8)
Cardiac devices*	–	19 (95.0)	39 (97.5)
No. Segments	155	308	541

Fig. 2. Results from a per-layer analysis (basal, mid-ventricular, apical) **(A),** and a per-segment analysis **(B)** of the median ECV values found across the entire study population.
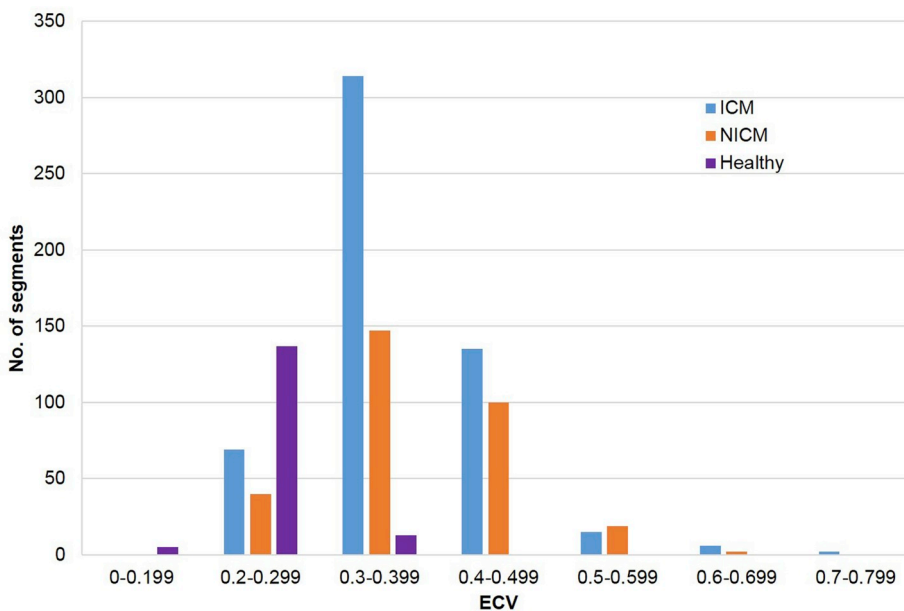

Fig. 3. Distribution histogram of all ECVs measured in the study. Overall, 88.4% (137/155) of the of healthy myocardium ECV measurements range from 20 to 29.99%; 80.2% (247/308) of the NICM ECVs range from 30 to 49.99%; and 83.0% (449/541) of ICM ECVs range from 30 to 49.99%.

myocardium and NICM, as well as ICM. 2) All of our subjects with CM present were imaged with a third-generation DSDE CT scanner, which has been shown to outperform second generation scanners for both single-source and DECT in the measurements of iodine concentration.[20] 3) In our study, ECV estimates were based on iodine measurements instead of Hounsfield Units (HU), which eliminates the need for a non-contrast acquisition (virtual or true). 4) A threshold to distinguish healthy myocardial tissue from CM had not been established to date.

The elimination of the need for a non-contrast scan using the DECT approach results in a decrease in radiation dose, in comparison to the
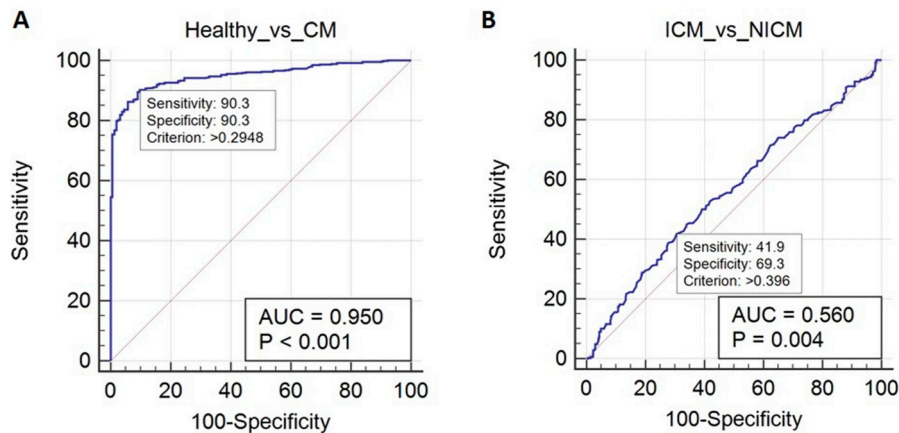
Fig. 4. Results from ROC curve analysis (with corresponding AUC) and Youden's index assessment to distinguish healthy myocardium ECVs from CM **(A).** Results from ROC curve analysis (with corresponding AUC) and Youden's index assessment to distinguish NICM ECVs from ICM **(B).**

SECT approach, while still providing similar results.[9] Using only one acquisition for the calculation of ECV also leads to a decrease in calculation time, which greatly improves the possibility of developing a fully automated ECV algorithm. Furthermore, the DECT approach avoids the mismatching error of drawing ROIs at different positions caused by the separate acquisition of the non-contrast and the contrast-enhanced delayed scan used in a SECT approach.

A CT approach to measure ECV is of particular interest in patients with metallic devices, since this population is often excluded from cardiac MRI examinations. Among the CM patients included in this study, 97% (58/60) had either pacemakers or implantable cardioverter defibrillator (ICD) wires at the time of their CT acquisition, resulting in metal artifacts. Metallic devices greatly influence the image quality of SECT datasets, causing severe beam hardening and photon starvation artifacts. Both of these artifacts are intrinsically related to the polychromatic nature of the single-energy x-ray beam used in SECT examinations. Strategies to reduce beam hardening artifacts rely on the development of specific algorithms and the use of higher tube potentials. These strategies come with several disadvantages such as an increase in radiation dose.[21–23] Compared to SECT acquisitions, DECT offers the possibility to evaluate scans at different kV levels and has the potential to reduce both beam hardening and metal artifacts[24–26]; this reduction in artifacts can be achieved via the simple post-processing procedure of adjusting the monoenergetic level to the optimal value.[27,28] Several studies in patients with metallic implants who underwent DECT showed that monoenergetic level optimization provided superior image quality and diagnostic value.[22,23]

There are some limitations to our study that merit consideration. First, we did not pursue a comparison with an MRI-based methodology, which is the reference standard for the noninvasive assessment of ECV; however, previous studies have shown that ECV can be successfully measured using a CT-based approach, with high correlation between ECV measurements derived from histologic quantification and equilibrium MRI.[4,8,10–12] Second, although a large number of segments were acquired for the analysis of healthy ECVs (155 ROIs), only 10 patients were included in the evaluation. A larger sample of healthy subjects might be necessary to further validate the study findings. Finally, it is important to note that the post-processing software "heart PBV", which is based on the 3-material decomposition method, is dependent on spectral separation and thus is system-specific; moreover, attenuation values have been shown to significantly vary between CT scanners of different manufacturers, or even among same manufacturers but different generation scanners.[20,29]

5. Conclusions

The findings of this study resulted in a statistically significant distinction between ECVs for healthy myocardium and CM ECVs. This led to the establishment of a promising threshold ECV value that could facilitate the differentiation between healthy and diseased myocardium, and highlights the potential of this methodology to detect cardiomyopathic tissue. It should be noted that the threshold value calculated in this study is not intended to be used as an absolute diagnostic test, but rather as a tool that could provide additional value for the characterization of myocardial tissue.

References

1. Wexler R, Elton T, Pleister A, Feldman D. Cardiomyopathy: an overview. *Am Fam Physician.* 2009;79:778.
2. Maron Barry J, Towbin Jeffrey A, Thiene G, et al. Contemporary definitions and classification of the cardiomyopathies. *Circulation.* 2006;113:1807–1816.
3. Ho CY, López B, Coelho-Filho OR, et al. Myocardial fibrosis as an early manifestation of hypertrophic cardiomyopathy. *N Engl J Med.* 2010;363:552–563.
4. Nacif MS, Kawel N, Lee JJ, et al. Interstitial myocardial fibrosis assessed as extracellular volume fraction with low-radiation-dose cardiac CT. *Radiology.* 2012;264:876–883.
5. Haaf P, Garg P, Messroghli DR, Broadbent DA, Greenwood JP, Plein S. Cardiac T1 mapping and extracellular volume (ECV) in clinical practice: a comprehensive review. *J Cardiovasc Magn Reson.* 2017;18:89.
6. Muscogiuri G, Suranyi P, Schoepf UJ, et al. Cardiac magnetic resonance T1-mapping of the myocardium. *J Thorac Imaging.* 2018;33:71–80.
7. Muscogiuri G, Gatti M, Dell'Aversana S, et al. Diagnostic accuracy of single-shot 2-dimensional multisegment late gadolinium enhancement in ischemic and non-ischemic cardiomyopathy. *J Thorac Imaging.* 2019. https://doi.org/10.1097/RTI.0000000000000402.
8. Bandula S, White SK, Flett AS, et al. Measurement of myocardial extracellular volume fraction by using equilibrium contrast-enhanced CT: validation against histologic findings. *Radiology.* 2013;269:396–403.
9. van Assen M, De Cecco CN, Sahbaee P, et al. Feasibility of extracellular volume quantification using dual-energy CT. *J. Cardiovasc. Comput. Tomogr.* 2019;13:81–84.
10. Lee H-J, Im DJ, Youn J-C, et al. Myocardial extracellular volume fraction with dual-energy equilibrium contrast-enhanced cardiac CT in nonischemic cardiomyopathy: a prospective comparison with cardiac MR imaging. *Radiology.* 2016;280:49–57.
11. Kurita Y, Kitagawa K, Kurobe Y, et al. Estimation of myocardial extracellular volume fraction with cardiac CT in subjects without clinical coronary artery disease: a feasibility study. *J. Cardiovasc. Comput. Tomogr.* 2016;10:237–241.
12. Nacif MS, Liu Y, Yao J, et al. 3D left ventricular extracellular volume fraction by low-radiation dose cardiac CT: assessment of interstitial myocardial fibrosis. *J. Cardiovasc. Comput. Tomogr.* 2013;7:51–57.
13. Abadia AF, Grant KL, Carey KE, Bolch WE, Morin RL. Spatial distribution of iron within the normal human liver using dual-source dual-energy CT imaging. *Investig Radiol.* 2017;52:693.
14. Graser A, Johnson TRC, Chandarana H, Macari M. Dual energy CT: preliminary observations and potential clinical applications in the abdomen. *Eur Radiol.* 2008;19:13.
15. Johnson TRC, Krauß B, Sedlmair M, et al. Material differentiation by dual energy CT: initial experience. *Eur Radiol.* 2007;17:1510–1517.
16. Nakahara T, Toyama T, Jinzaki M, et al. Quantitative Analysis of Iodine Image of Dual-energy Computed Tomography at Rest: comparison with 99mTc-tetrofosmin

stress-rest single-photon emission computed tomography myocardial perfusion imaging as the reference standard. *J Thorac Imaging.* 2018;33:97–104.

17. Ruzsics B, Lee H, Powers Eric R, Flohr Thomas G, Costello P, Schoepf UJ. Myocardial ischemia diagnosed by dual-energy computed tomography: correlation with single-photon emission computed tomography. *Circulation.* 2008;117:1244–1245.

18. Dabir D, Child N, Kalra A, et al. Reference values for healthy human myocardium using a T1 mapping methodology: results from the International T1 Multicenter cardiovascular magnetic resonance study. *J Cardiovasc Magn Reson.* 2014;16:69.

19. Sado DM, Flett AS, Banypersad SM, et al. Cardiovascular magnetic resonance measurement of myocardial extracellular volume in health and disease. *Heart.* 2012;98:1436–1441.

20. Euler A, Solomon J, Mazurowski MA, Samei E, Nelson RC. How accurate and precise are CT based measurements of iodine concentration? A comparison of the minimum detectable concentration difference among single source and dual source dual energy CT in a phantom study. *Eur Radiol.* 2019;29:2069–2078.

21. Watzke O, Kalender WA. A pragmatic approach to metal artifact reduction in CT: merging of metal artifact reduced images. *Eur Radiol.* 2004;14:849–856.

22. Bamberg F, Dierks A, Nikolaou K, Reiser MF, Becker CR, Johnson TR. Metal artifact reduction by dual energy computed tomography using monoenergetic extrapolation. *Eur Radiol.* 2011;21:1424–1429.

23. Meinel FG, Bischoff B, Zhang Q, Bamberg F, Reiser MF, Johnson TR. Metal artifact reduction by dual-energy computed tomography using energetic extrapolation: a systematically optimized protocol. *Investig Radiol.* 2012;47:406–414.

24. Johnson TR. Dual-energy CT: general principles. *Am J Roentgenol.* 2012;199:S3–S8.

25. Yu L, Leng S, McCollough CH. Dual-energy CT–based monochromatic imaging. *Am J Roentgenol.* 2012;199:S9–S15.

26. Vliegenthart R, Pelgrim GJ, Ebersberger U, Rowe GW, Oudkerk M, Schoepf UJ. Dual-energy CT of the heart. *Am J Roentgenol.* 2012;199:S54–S63.

27. Tabari A, Lo Gullo R, Murugan V, Otrakji A, Digumarthy S, Kalra M. Recent advances in computed tomographic technology: cardiopulmonary imaging applications. *J Thorac Imaging.* 2017;32:89–100.

28. Lenga L, Albrecht MH, Othman AE, et al. Monoenergetic dual-energy computed tomographic imaging: cardiothoracic applications. *J Thorac Imaging.* 2017;32:151–158.

29. Birnbaum BA, Hindman N, Lee J, Babb JS. Multi–detector row CT attenuation measurements: assessment of intra-and interscanner variability with an anthropomorphic body CT phantom. *Radiology.* 2007;242:109–119.